

Chiplet Cloud: Building AI Supercomputers for Serving Large Generative Language Models

Huwan Peng
hwpeng@uw.edu
University of Washington

Scott Davidson
stdavids@uw.edu
University of Washington

Richard Shi
cjshi@uw.edu
University of Washington

Shuaiwen Leon Song*
shuaiwen.song@sydney.edu.au
The University of Sydney

Michael Taylor
prof.taylor@gmail.com
University of Washington

Abstract

Large language models (LLMs) such as OpenAI’s ChatGPT and Google’s Gemini have demonstrated unprecedented capabilities of autoregressive AI models across multiple tasks triggering disruptive technology innovations around the world. However, as models continue to grow the cost to serve these models also continues to grow threatening the democratization of LLMs.

To address this issue, we propose *Chiplet Cloud*, a chiplet-based ASIC LLM-supercomputer architecture whose goal is to optimize the total cost of ownership (TCO) per generated token. This architecture is a highly parameterizable ASIC and server-level architecture leveraging thousands of replicated accelerator modules collaborating to scale-up the performance of LLMs at cloud-scale. To determine specific parameterizations of the Chiplet Cloud architecture, we implemented a two-phase hardware-software co-design methodology that can search the massive design space and fine tune the architecture across a collection of LLMs based on an accurate inference simulation. A common bottleneck for LLMs is the memory access performance therefore we introduce CC-MEM, a scalable on-chip memory system for Chiplet Cloud architectures. Using the CC-MEM, Chiplet Clouds can be built using only SRAMs for design points where the power and performance of memory access is critical. The CC-MEM also includes a compression decoder module to add support for sparse models without impacting the compute units using a Store-as-Compressed, Load-as-Dense mechanism.

We evaluate Chiplet Cloud architectures across eight popular LLMs on the market representing a variety of model sizes. Using fine tuned Chiplet Cloud servers we are able to achieve 97× and 18× improvement in TCO/Token over rented GPU and TPU clouds, or a 8.3× and 3.7× improvement over fabricated GPU and TPU clouds respectively. Chiplet Cloud can also support 1.7× larger models with a sparsity of 60%.

1 Introduction

Recently, generative Large Language Models (LLMs) like ChatGPT [35] have gained significant attention around the world due to their unprecedented ability to perform a variety of natural language tasks. These LLMs are currently driving a technology revolution at planet-scale, changing the way we interact with AI models on a daily basis from web search, word processing, and programming [16].

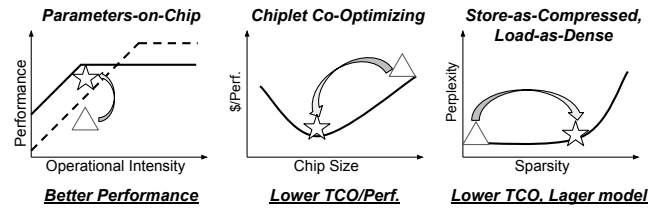


Figure 1: Compared to conventional systems, Chiplet Cloud (1) fits all model parameters inside the on-chip CC-MEM, greatly improving the performance; (2) co-optimizes the chip size with software mapping to reduce TCO/Perf; (3) exploits sparsity to reduce TCO and support larger models.

A major contributing factor to the increase in ML capabilities comes from the unprecedented scale of the LLMs being deployed. Most LLMs used today have billions [8, 9, 55] or even trillions of parameters [13]. Serving modern generative LLMs on commodity hardware, like GPUs, is already hitting a *scalability wall*. For example, Google Search is estimated to process over 99,000 queries [30] per second while state-of-the-art GPT-3 throughput on GPUs is 18 tokens/sec per A100 [3]. If GPT-3 is embedded into every query and each query generates 500 tokens, Google would need 340,750 NVIDIA DGX servers (2,726,000 A100 GPUs) to keep up. Assuming every GPU was able to sustain 50% utilization, the average power would be over 1 Gigawatt which is enough energy to power 750,000 homes [11]. To address these scalability issues, we must design hardware systems that attain significantly better *total-cost-of-ownership (TCO) per token served*.

We propose *Chiplet Cloud*, a highly parameterizable chiplet-based ASIC LLM-supercomputer architecture which aims to reduce TCO per generated token. The main insights behind the Chiplet Cloud architecture are shown in Figure 1. To address the potential bandwidth bottlenecks of LLM inference, the Chiplet Cloud architecture allows for all model parameters and KV values to be stored in a memory system called CC-MEM (Section 3.1), a scalable on-chip memory system for Chiplet Cloud architectures. We use a finely tuned replicated chiplet accelerator module to reduce the fabrication cost as we scale the system to meet performance demands (Section 3.3). To support models that leverage sparsity, we use a compression decoder unit which lives within the CC-MEM network to implement a *Store-as-Compressed, Load-as-Dense* mechanism (Section 3.2). We show these design choices win in

*Work done prior to affiliation with Microsoft

the competition of TCO per token for serving generative LLMs but requires careful consideration with respect to the chiplet die size, chiplet memory capacity and bandwidth, and total number of chiplets to balance the fabrication cost and model performance (Section 2.3 and Section 3.4).

To explore the massive hardware-software co-design space of Chiplet Cloud and find TCO per token optimal parameterizations, we propose a two-phase design-search methodology that fine tunes the architecture across a collection of LLM workloads. The hardware exploration phase (Section 4.1) conducts a bottom-up design space exploration of Chiplet Cloud hardware architecture from a flexible accelerator architecture up to a 1U rack mounted server architecture taking power budget, floorplan, and thermal constraints into account. The software evaluation phase (Section 4.2) then performs a detailed performance and TCO analysis of the server designs given a specific workloads while simultaneously searching for a software mapping strategy that complements the server architecture. While software mapping strategies for LLMs are now considered standard techniques for improving performance on existing hardware platforms, our design methodology flips the order and allows us to explore mapping strategies across all possible Chiplet Cloud hardware configurations for a software-hardware co-design methodology.

In summary, this paper makes the following contributions:

- We propose *Chiplet Cloud*, a chiplet-based ASIC LLM supercomputer with a dedicated memory system architecture CC-MEM for serving generative LLMs designed to improve the TCO/Token over currently deployed systems (Section 3.1, Section 3.3);
- We design a compression decoder unit in the CC-MEM network and propose the store-as-compressed, load-as-dense mechanism to support sparsity enabled LLMs (Section 3.2);
- We present a comprehensive software-hardware co-design methodology¹ that enables an accurate Chiplet Cloud design space exploration with software mapping optimization aware search (Section 4);
- We design and evaluate the Chiplet Cloud architecture across eight popular LLMs representing a variety of model sizes (Section 5). Compared to running on rented GPU and TPU clouds, Chiplet Cloud can achieve up to 97× and 18× improvement in TCO/Token (Section 6).

2 Background

2.1 Large Generative Language Models

While generative LLMs have undergone many improvements, the model’s architecture, shown in Figure 2, has remained relatively unchanged. These models are constructed by stacking layers of transformer decoder blocks [57] which are composed of a self-attention mechanism followed by a 2-layer feed-forward network. The number of compute operations for each step of the decoder block is shown in Figure 2. In modern LLMs, the fully-connected (FC) layers often dominate the runtime since the model dimension d is significantly larger than the context length l_{ctx} , thus $O(ld^2) \gg$

¹The methodology is packaged as a design tool that can be shared to the community and is applicable to other cloud architectures.

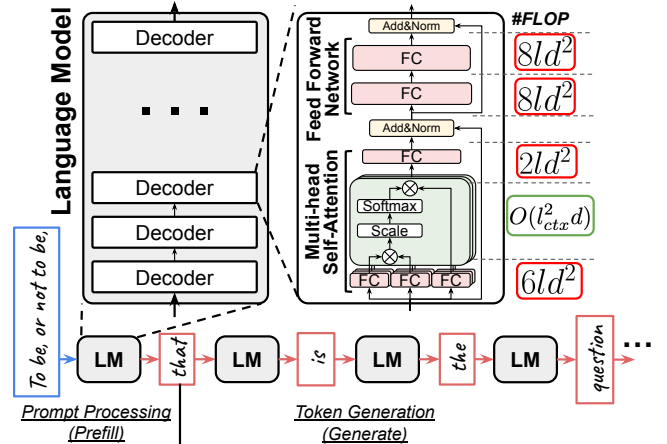


Figure 2: General architecture of an autoregressive generative large language model. In most LLMs, d is significantly larger than l_{ctx} , causing FC layers to dominate the overall runtime. The inference is partitioned into two stages: prompt processing (prefill) and token generation (generate).

$O(l_{ctx}^2d)$. For example, in GPT-3, where $d = 12288$ and $l_{ctx} \leq 4096$, more than 99% of MAC operations are performed in the FC layers.

Generative LLM models employ autoregressive inference, as visualized in the lower part of Figure 2. This inference process unfolds in two stages: prompt processing, or *prefill*, and token generation, or *generate*. In the prefill stage, the model ingests the entire input sequence to generate the initial output token. In the generate stage, this output token serves as the input for subsequent passes, producing new tokens iteratively. This iterative process continues until a specific "end of text" token is generated or the sequence reaches a predefined maximum length. This research centers on optimizing token generation, which typically consumes significantly more time than the prefill phase and incurs a higher cost per token [35].

Since the appearance of the original transformer architecture [57], the development of LLMs has mainly focused on dimension scaling, such as layer size and number of layers. LLMs may also have different operations, such as activation function (ReLU [1], GeLU [18], Swish [44] and their GLU variants [47]), positional embeddings (absolute [57], relative [45], ALiBi [40] and RoPE [51]), and normalization (original layer normalization [4] and RMS layer normalization [61]).

2.2 Main Challenges

2.2.1 Memory Bandwidth Significantly Limits Inference Performance Inference performance of a LLM, both latency and throughput, is often bottlenecked by memory bandwidth. The FC layers are plagued with low operational intensity leading to memory bounded operation for a majority the model [3]. A prevalent strategy for enhancing throughput involves employing a large batch size, thereby improving the operational intensity of the FC layers but at the cost of an increase in prefill latency and KV cache size. For example, a GPT-3 model with a context length of 2K would require 2 GB for the KV cache. *KV caching* is a widely adopted technique in

token generation, where intermediate results of the self-attention mechanism from previous input tokens are cached, eliminating the need for recomputation. With a batch size of 256, the KV cache grows to 512 GB while the total model parameter size is 350 GB. Reducing parameter and KV access latency and power is critical for achieving a good cost per throughput (i.e. TCO/Token).

2.2.2 Chip Costs Dominate TCO The autoregressive nature of LLMs severely constrains hardware utilization. The best hardware utilization on the state-of-the-art implementation is around 50% [3] on GPUs and 40% on TPUs (during the decoding phase) [37]. It is noteworthy that these are achieved with a very large batch size (e.g. 1024) as the utilization can be as low as 1% when batch sizes are small (e.g. 4) [37], which is a common case for real-world LLM inference. Compounding this issue is the massive scale of contemporary chips (e.g. A100 GPU), approaching the wafer reticle limit of around 800 mm², presenting a huge challenge in managing fabrication costs. Under conditions of low utilization and high chip fabrication costs, capital expenditures (CapEx) become a substantial fraction of the TCO. Our evaluation indicates that at 50% utilization, the TCO of running an A100 GPU purchased at manufacturer’s retail price is 97.7% CapEx. Even in scenarios where individuals tapeout their own GPUs, the CapEx percentage can remain as high as 58.7%. The pivotal strategy for reducing TCO per generated token therefore involves addressing the challenge of capital expenditure.

2.3 Architectural Solutions

To build ASIC supercomputers for LLMs that effectively address these challenges, this paper explores an architectural solution within the following two design spaces.

2.3.1 New Memory System for Better Performance and TCO In situations where we are bottlenecked on memory bandwidth, our focus is to mitigate the reliance on external memory solutions such as HBM or DDR by allowing the architecture to buffer all model parameters and intermediate data (such as the KV cache) in an on-chip memory system using SRAM. SRAM can have a much higher bandwidth and much lower access energy, albeit at the cost of lower storage density. Recently, there has been an industry trend to deploy more on-chip memory on deep learning accelerators to reduce the excessive off-chip memory access. Microsoft’s Brainwave [14] pins DNN model weights in distributed on-chip SRAM. Google’s TPU v4i [20] and TPU v4 [19] contains 144 MB and 177 MB SRAM respectively, and GraphCore’s IPU 2 [25] has 896 MB SRAM. While SRAM has better performance and access energy, it is more expensive per bit thus an exploration is required to determine if SRAM only systems are superior with respect to TCO/Token.

2.3.2 Chiplet for Reducing Fabrication Cost An extreme case of adding on-chip memory is to go wafer-scale. Cerebras WSE-2 [52] is a 46,255 mm² chip with 40 GB on-chip memory. The niche wafer-scale designs are expensive to manufacture, resulting in limited potential for TCO reduction. We advocate for the incorporation of chiplet technology as a pivotal strategy for managing TCO for LLM supercomputers. Chiplet technology has recently become a new trend in the industry. It breaks down a traditional monolithic silicon chip into multiple small chiplets and integrates them into a single package. This approach improves fabrication yield, reduces

manufacturing costs and enables die-level reuse for different system scales. For TSMC 7nm technology with a defect density of 0.1 per cm², the unit price of a 750 mm² chip is twice that of a 150 mm² chip. It is currently an available commodity technology that all architects can use, aligning with our TCO/Token optimization focus.

One potential drawback of chiplet design is the high inter-chiplet communication. Studies on GPUs and TPUs have shown that proper mapping strategies (e.g. tensor and pipeline parallelism [33, 37, 48]) can effectively reduce the inter-node communication. Recent research [37] proposes a *2D weight-stationary layout* to partition the feed-forward network. Compared with conventional 1D partitioning, this method makes the communication time of the feed-forward networks scale as $O(\frac{1}{\sqrt{n_{chips}}})$. Systems with more chiplets benefit from this approach over systems with fewer monolithic chips.

One question in harnessing chiplet technology pertains to identifying packaging techniques that align with our design goals of reducing TCO/Token. Two widely adopted solutions are silicon interposers [22] and organic substrates [32]. Silicon interposers provide higher signal density for high bandwidth and is a key component for HBM integration. However, it has a limited max signal distance and adds significant unit cost. In scenarios where HBM is not employed, organic substrates could be a better choice offering a more economically viable TCO/Token.

3 Chiplet Cloud: A TCO-Optimized ASIC Supercomputer Architecture for LLMs

Accelerator designs often focus on raw hardware performance, however this is not always aligned with cloud hardware designers whose systems are optimized for TCO per performance [20]. TCO includes both the capital expenditure (*CapEx*) plus the operation expenditure (*OpEx*) over the lifetime expectancy of the system (*Life*), giving us the equation $TCO = CapEx + Life \times OpEx$. Optimizing TCO is therefore a balance of how much you are willing to pay for the additional performance. Aiming for improved TCO per performance, we propose a chiplet-based cloud-scale system design for LLM inference, called **Chiplet Cloud**. The architectural breakdown of Chiplet Cloud is shown in Figure 3, which includes the high-level abstract architecture at different levels from the memory system up to the chiplet module, server, and cloud.

3.1 Chiplet Cloud Memory Architecture

The heart of Chiplet Cloud is the Chiplet Cloud Memory architecture CC-MEM (Figure 3 (a)). CC-MEM is a scalable on-chip memory system with the ability to sustain high-bandwidth, low-latency read and write operations. This is the main memory for each chiplet in the chiplet-cloud system which stores the model parameters, KV cache and activations.

The CC-MEM is designed to act as a drop-in replacement for DRAM memory but leverages SRAM to give us opportunities to take advantage of higher-bandwidth and lower-latency memory access for significantly better performance for the low operational intensity kernels of LLMs. SRAMs are clustered into bank groups with each bank group acting as a virtual single-port memory. Each bank group also contains a compression decode unit including a sparse tile memory.

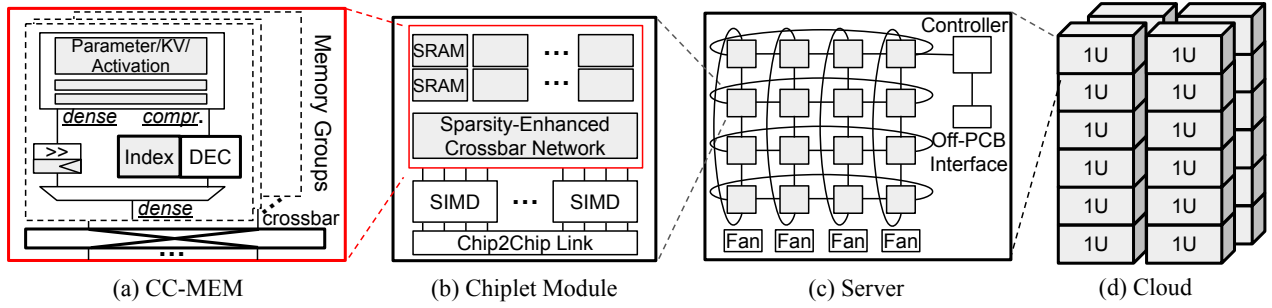


Figure 3: Chiplet Cloud architecture from the CC-MEM to the cloud.

Bank groups are interconnected using a pipelined crossbar switching network. The decision to use a crossbar network comes from the low-latency and low-global communication power overhead while being able to achieve a 100% saturated throughput with reasonable network scheduling. The biggest downside of utilizing a crossbar network comes from their area scalability as the network scales quadratically with the radices of the network. As with many networks, this area is routing dominated. The CC-MEM is mostly SRAM; thus, there is an abundance of routing tracks available above the SRAM devices severely lessening the area overhead of crossbar network, a concept known as *NoC symbiosis* [36]. Crossbar networks also have the benefits of being simple to model both in terms of latency (pipeline depth) and congestion (bank conflicts). This allows our hardware-software co-design search space to take into account memory scheduling to ensure that we can achieve the memory access performance that is required in order to hit our target TCO/performance metrics.

The CC-MEM supports burst mode operations. Each bank group contains a simple control unit to facilitate in bursting multiple sequential read/write commands within a bank group. This control unit is programmed using simple memory mapped control status registers. Due to the highly structured nature of GEMM kernels, burst mode operations will make up a majority of the memory operations during moments of computation and will greatly reduce the burden on the compute unit to keep the memory system bandwidth at near-peak throughput.

3.2 CC-MEM for Sparsity

There is a growing interest in reducing LLM inference costs via model compression. Recent work [15] has shown that large models are more compressible and have significantly less accuracy drop off than small models under compression. OPT-175B [62], which has the same model architecture as GPT-3, can reach 60% unstructured sparsity with negligible increase in perplexity while requiring no fine-tuning effort. Supporting unstructured sparse model on ASIC can be challenging since the highly irregular sparsity can lead to unpredictable data access and compute patterns. Simultaneously, sophisticated decoder and on-chip network architecture for sparse data dispatching can add significant area overhead. To address these issues, we implement a *Store-as-Compressed, Load-as-Dense* mechanism into the CC-MEM architecture. Models are compressed using a tile-based compressed sparse row format [34] and stored in the

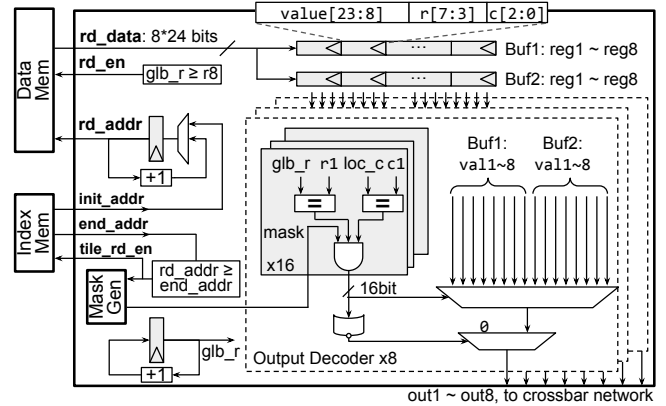


Figure 4: Compression decoder unit.

CC-MEM in this sparse format. However, load access patterns and data appear as if the data was stored dense. The methodology is based on the insight that *TCO/Token of our proposed system will be primarily limited by the on-chip memory size, rather than memory bandwidth and compute unit utilization*. Reducing the required memory size will be the first priority when supporting sparse models. Using this mechanism, the compute units are *sparsity-agnostic* and do not require any special design, reducing area overhead and increasing flexibility.

To support this methodology, each bank group within the CC-MEM contains a compression decode unit. Data in CC-MEM can be in raw dense formats or sparse compressed formats. The decode units are controlled using a simple set of memory mapped CSRs similar to the burst mode CSRs. Data sent over the network is always in dense formats, allowing any network attached compute units to be completely agnostic to the format the data is stored in. Compressed data ultimately has a lower bandwidth than dense data. This is because dense data and sparse data are both stored in the same SRAM banks which have the same peak bandwidth but sparse data has additional bits per word.

Figure 4 shows an example design of the compression decoder unit. In this example, the sparse matrix is divided into tiles of shape (32, 8). Like the standard compressed sparse row format, non-zero values (NZV, 16 bits) in a tile are encoded using a 5-bit row index (r) and a 3-bit column index (c), forming a 24-bit sparse word stored in

data memory. Tile indexes are stored in a separate index memory, which is placed together with crossbar routing tracks to minimize area overhead. To read sparse data, the decoder sends a tile read request to the index memory and receives the initial address and end address of the NZVs in a tile. The decoder then reads data memory at a rate of up to 8 sparse words per cycle and writes them to a double-buffer. Depending on the row index and column index, zeros are inserted accordingly to form the original dense tile. The unit can constantly output 8 dense words per cycle.

3.3 From Chiplet to Cloud

Figure 3 (b) shows a LLM accelerator chiplet module. Inside the chiplet, multiple SIMD cores are attached to a CC-MEM. Compared to a fully custom compute units, the SIMD cores are more flexible with very few limitations on the types of kernels that can be efficiently supported, which is essential for supporting the various activation functions and embeddings found in modern LLMs.

In Chiplet Cloud, a single chiplet module functions as a discrete package, with multiple chiplets interlinked across the board. Advanced package-level solutions such as the silicon interposers [22] can provide higher signal density for high bandwidths in-package communication. However, it has a limited reach and adds more cost. In contrast, our Chiplet Cloud design adopts a *board-level* organic substrate chiplet approach, aligning with specific communication requirements. Given the large scale of modern LLMs, running the model within a single package of chiplets is often impractical. Partitioning into multiple packages or even across servers becomes a necessity. This partitioning mandates collective operations, such as all-reduce, to occur across packages. Since the conventional ring all-reduce implementation is limited by the slowest link among nodes, the in-package high-speed links do not provide much help in this case. Compared to conventional package-level chiplet, the board-level chiplet architecture eliminates cost of advanced packaging.

Each Chiplet Cloud server (Figure 3 (c)) contains a printed circuit board (PCB) with multiple chiplets, a controller and an off-PCB network interface. The controller, which can be an FPGA or a microcontroller, dispatches remote procedure calls from off-PCB interface to all chiplets. Chiplets are connected together via a 2D torus on-PCB network, which is able to accommodate the many different mapping strategies that we might need to implement to efficiently run different models. Candidates for chip-to-chip interfaces can be custom-designed links such as NVIDIA ground-referenced signaling GRS links [38, 56], Google TPU’s Inter-Core Interconnect [21], Graphcore’s IPU-links [25], or high-speed PCI-e which has been widely used as interconnects for many deep learning chips [28, 39, 49]. Off-PCB interfaces could be 10/100 Gigbit Ethernet or InfiniBand, enabling communication between adjacent servers.

3.4 Design Space Discussion

The design space of Chiplet Cloud is a balancing act that includes many different architectural parameters across the entire system that greatly impact the resulting TCO/Token. Some aspects include (1) *Chiplet Module Size*: small chips benefit from higher yields while incurring more per-chip overhead; (2) *Per Chiplet Memory*

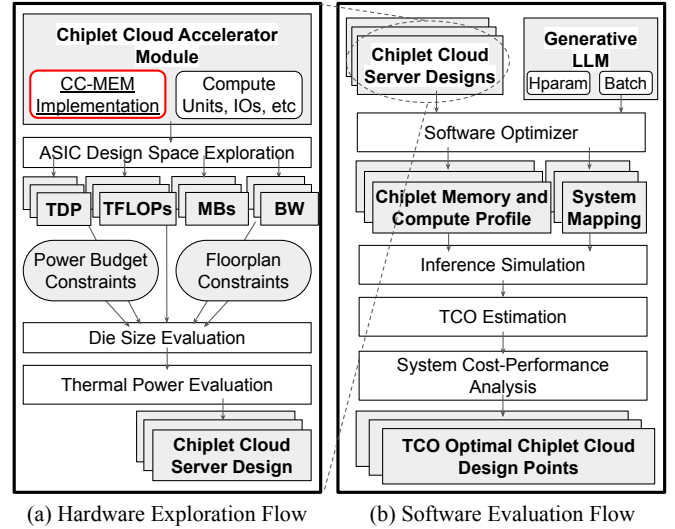


Figure 5: Two phase design methodology flow diagram. (a) The hardware exploration flow performs a bottom-up, LLM agnostic design space exploration generating thousands of realizable Chiplet Cloud server designs. (b) The software evaluation flow then takes the realizable server design points along with a generative LLM specification to perform software optimized inference simulations and TCO estimations to find the optimal Chiplet Cloud design points.

Size: more memory on chips means few chips required but few FLOPS per chip; (3) *Per Chiplet FLOPS*: more FLOPS increases performance while requiring higher memory bandwidth, resulting in a larger memory crossbar; and (4) *Software Mapping*: the trade-off between different parallelisms affects utilization and interconnect data communication. Since all of these aspects are tightly coupled, a comprehensive design methodology is critical to optimize the end-to-end performance and TCO.

4 Chiplet Cloud Design Methodology

The design methodology for Chiplet Cloud, shown in Figure 5, is a critical component for finding design points with best-in-class TCO/Token. When we scale to the size of cloud supercomputers, small changes at the architecture level have massive implications at the warehouse scale over the lifetime deployment of the system. We there take a brute-force approach to the design space exploration which eliminates any preconceived assumptions and allows the models to decide what is the best hardware-software design pair.

4.1 Phase 1: Hardware Exploration

The hardware exploration phase of the Chiplet Cloud design methodology (as shown in Figure 5(a)) is a bottom-up, LLM agnostic, design space exploration resulting in *tens of thousands* of feasible Chiplet Cloud server designs. This exploration manifests as a substantial parameterization sweep, guided by multi-level hardware specifications provided as input, and user-preconfigured constraints and

constants. Some essential parameters are listed in Table 1. Throughout the hardware exploration, every conceivable combination of input values undergoes evaluation, spanning diverse parameters like chip performance, SRAM size, and variations in the number of chiplets within servers.

ASIC Design Space Exploration. Since our optimization target is TCO/Token, the 3 most critical estimations that need to be performed are the silicon area, power consumption, and end-to-end performance, as these are the 3 biggest contributors to capital-expenditure, operational-expenditure, and tokens-per-second respectively. The silicon area, energy per operation, memory bandwidth, and peak power draw of the design are estimated during the hardware exploration phase, and the end-to-end performance is evaluated in the software evaluation phase with a specific application.

Die Size Evaluation. The die area modeling is separated into memory, compute, and auxiliary components. For memory, we use the CC-MEM architecture described in Section 3.1, including multiple SRAM banks, sparse decoders, and a crossbar network. It was modeled using a 12nm implementation, which is synthesized, placed and routed using Synopsys Design Compiler and Synopsys IC Compiler II. These results were then scaled to 7nm using 2 scaling factors, one for area attributed to SRAM bitcells which uses the reported High-Density SRAM bitcell area values for 7nm and one scaling factor for routing dominated area which uses reported contacted-poly-pitch by minimum-metal-pitch (CCP-MMP) [60]. The CC-MEM is routing dominated in regions that are not SRAM therefore we do not need to take into consideration transistor scaling. The computation and auxiliary component area modeling and constraints are derived from publicly available information on 7nm NVIDIA A100 GPU [54]. Compared to a fully custom accelerator designs that are prolific in the literature, the A100 is a more flexible offering with very few limitations in the types of kernels it can operate efficiently on, which is essential for supporting various activation functions and positional embeddings, as introduced in Section 2.1.

Thermal Power Evaluation. The power model is also derived from A100 GPU. We normalize the TDP and peak performance to W/FLOPS and use that value to model our Chiplet Cloud accelerator. This is a simple and conservative estimate since a significant portion of GPU power comes from DRAM, but it greatly simplifies the power model and increases the confidence interval of our TCO/Token modeling results. Combined with the area model, we limit the chip power density to be no more than 1 W/mm². On the server level, we will further refine the peak power density limitations based on the full-server thermal analysis, and eliminate any thermally infeasible designs.

4.2 Phase 2: Software Evaluation

The second phase of the design methodology models the execution time of specific workloads across the hardware design points and searches for optimal Chiplet Cloud architectural configurations, as shown in Figure 5(b).

Software Optimizer. In this stage, we conduct software optimizations, incorporating *tensor parallelism* and *pipeline parallelism*

Table 1: Essential parameters of Chiplet Cloud hardware exploration

Parameters	Range
Technology	7nm
Die Size	20 mm ² to 800 mm ²
Memory Density	Scaled from 12nm implementation
Memory Bandwidth	Scaled from 12nm implementation
Compute Density	2.65 mm ² /TFLOPS
Power Density	1.3 W/TFLOPS, <1W/mm ²
Chip IO	25 GB/s * 4 links
Wafer Defect Density	0.1 / cm ²
Wafer Cost	\$10000
Server Size	1u, 19 inch
Lanes per Server	8
Silicon per Lane	<6000 mm ²
Chips per Lane	1 to 20
Power per Lane	<250 W
Server Thermal	Adapted from ASIC Clouds [29]
PSU Efficiency	0.95
DCDC Efficiency	0.95
Ethernet	100 Gigabit, \$450
Server Life	1.5 year

with microbatch tuning [33, 48]. It will first look at the hyper-parameters of the LLM, such as the model dimension d_{model} , number of layers, context length, attention mechanism type (multi-head or multi-query), as well as expected batch size. Then it will decompose the full model into a collection of small kernels that can be mapped to the individual chiplets throughout the system. In cases where the model cannot fit into a single server, the server will be replicated to scale up the entire system until there are enough resources to execute the application. This results in a system mapping which has the portion of the model that each chiplet in the whole system will be responsible for executing. There also exists a chiplet memory profile (required memory for weights, activations, and the KV cache) and chiplet compute profile (operation type and size) for the portion of the model that will be running on the individual chiplet, which will allow us to accurately model the end-to-end performance of the full system.

Inference Simulation. The comprehensive end-to-end inference simulation for the Chiplet Cloud system initiates with an analytical analysis of the compute kernel, derived from the compute profile, and memory access kernel, derived from the memory profile. The size and configuration of these operations are scrutinized at the microarchitectural level to determine the corresponding latencies and energy. Given the system’s distributed nature across multiple chiplets, it becomes imperative to model data communication overhead, including all-reduce operations latency and energy. The latency of an all-reduce operation involving B bytes of data across N nodes is disassembled into one reduce-scatter and one all-gather operation, both sharing the same latency

$$T_{reduce-scatter} = (N - 1) \frac{D/N}{B} + T_{init}$$

where B denotes the bandwidth of the slowest connection among the nodes, and T_{init} represents the time required to initialize the operation.

Summing the latencies of all kernels and communications yields the latency of a single micro-batch inference. The subsequent step involves determining the end-to-end latency and throughput. Aligning with the pipeline schedule and micro-batching strategy akin to DeepSpeed Inference [3], we aim to enhance system utilization and mitigate pipeline bubbles, as depicted in Figure 6. Assuming a micro-batch latency denoted as l_{mb} and a pipeline stage latency of l_s , with a total of n micro-batches in consideration, the per-token latency during generation is constrained by both l_{mb} and the product of the micro-batch count and the pipeline stage latency, i.e., nl_s . The overall latency for generating t tokens is given by the formula:

$$l_{all} = l_{prefill} + (t - 1) \max(l_{mb}, nl_s)$$

The throughput for a batch size N is expressed as

$$\begin{aligned} throughput &= Nt/l_{all} \\ &= \frac{Nt}{l_{prefill} + (t - 1) \max(l_{mb}, nl_s)} \\ &\approx \frac{N}{\max(l_{mb}, nl_s)} \end{aligned}$$

Given that the total generation time is often significantly longer than the prefill time, and the token count t is typically substantial, we can neglect these factors. Therefore, the thoughtful selection of pipeline parallelism and micro-batching scheduling strategies is crucial for sustaining high system utilization and concurrently improving both latency and throughput.

In the context of systems like Chiplet Cloud, assuming a unit generation latency for batch size $N = 1$ and pipeline $p = 1$ as τ , and recognizing that the system is often compute-bound, the micro-batch latency is expressed as $l_{mb} = \frac{N}{n}\tau$, and the single stage latency becomes $l_s = \frac{l_{mb}}{p} = \frac{N}{np}\tau$. For a given system and batch size N , our objective is to determine the pipeline stages p and micro-batch counts n that maximize throughput. This is achieved by minimizing the expression

$$\begin{aligned} \arg \min_{n,p} \max(l_{mb,g}, nl_{s,g}) &= \arg \min_{n,p} \max\left(\frac{N}{n}\tau, \frac{N}{p}\tau\right) \\ &= \arg \min_{n,p} \max\left(\frac{1}{n}, \frac{1}{p}\right) \end{aligned}$$

Subject to the constraints $n \leq N$ and $p \leq \#layers$. Consequently, our goal is to maximize both p and n to optimize throughput. Hence, it is limited by the minimum of the number of layers and the batch size N . While it is acknowledged that practical considerations, such as communication latency and hardware inefficiencies, may introduce deviations from this idealized scenario, our approach provides a valuable starting point for exploring optimal mapping strategies.

TCO Estimation. The TCO model is based the model by Barroso et al [6], which includes both capital expenditures (*CapEx*) and operating expenses (*OpEx*) from the system as well as the data-center hosting the system. The *CapEx* includes the silicon die cost, package cost, PCB cost, power supply unit cost, heatsink cost, fan costs, Ethernet controller cost, and control processor cost. The *OpEx*

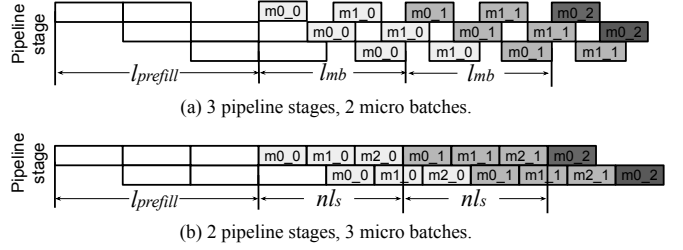


Figure 6: Diverse scheduling strategies for pipeline-parallelism and micro-batching. White boxes represent prompt processing (prefill), while shaded boxes denote token generation. The token generation throughput can be constrained either by (a) the micro-batch latency l_{mb} or (b) the product of the micro-batch count and the pipeline stage latency nl_s .

is calculated based on the power consumption of the system. Based on the system TDP and utilization from inference simulation, the full system average power consumption is used to determine the power draw from the silicon dies of the Chiplet Cloud accelerators. To estimate the die cost, we first calculate the number of fully patterned dies per wafer (DPW). This is the number of rectangular dies with the given die size dimensions that we can slice out of a traditional 300mm circular wafer. Cost per die is then calculated as

$$cost_{die} = \left(\frac{cost_{wafer}}{DPW} + cost_{test}\right)/Y_{die}$$

Where $cost_{wafer}$ is wafer price, $cost_{test}$ is testing cost, and Y_{die} is die yield. We use the classical negative binomial model [12] for yield which is as follow

$$Y_{die} = \left(1 + \frac{AD_0}{\alpha}\right)^{-\alpha}$$

Where A is die area, D_0 is defect density and α is cluster parameter. Since manufacturing yields drop with chip area, it makes economic sense to design smaller chips.

System Cost-Performance Analysis. The end-to-end performance and the corresponding TCO are fed into the system cost-performance analysis engine, where we compute all TCO related metrics and output the optimal design points under different hardware and software constraints.

4.3 Generalizing the Design Methodology

While this work is focused on trying to find cloud-scale architectures with best-in-class TCO/Token performance, the methodology of designing scale-up cloud systems is still applicable to existing ASIC architectures or architectures designed for programmable devices such as CGRAs or FPGAs. Given an appropriate power, performance and area estimation model for the accelerator module, this methodology is applicable.

5 Case Studies

To evaluate Chiplet Cloud and the design methodology, we performed a case study on eight language models, including GPT-2 [41], Megatron-LM [48], GPT-3 [8], Gopher [42], MT-NLG [50],

Table 2: TCO/Token optimal Chiplet Cloud systems for different language models.

Model	GPT-2 [41]	Megatron [48]	GPT-3 [8]	Gopher [42]	MT-NLG [50]	BLOOM [7]	PaLM [9]	Llama-2 [55]
Parameters (B)	1.5	8.3	175	280	530	176	540	70
d_{model}	1,600	3,072	12,288	16,384	20,480	14,336	18,432	8,192
Layers	48	72	96	80	105	70	118	80
Die Size (mm ²)	60	40	140	100	160	120	100	80
MB per Chip	32.8	27.0	225.8	151.0	198.0	137.5	95.0	82.5
TFLOPS per Chip	5.60	2.87	5.50	4.83	6.32	7.02	12.07	7.62
BW per Chip (TB/s)	2.80	2.29	2.75	2.41	4.21	3.51	1.51	1.90
Chips per Server	128	144	136	160	160	152	120	72
Number of Servers	24	8	96	80	105	70	118	80
Tensor Parall. Size	64	144	136	160	160	152	120	72
Pipeline Parall. Size	48	8	96	80	105	70	118	80
Batch Size	128	8	256	128	128	128	1024	512
Micro-Batch Size	2	1	2	2	1	2	8	4
Max Context Length	16K	256K	8K	16K	16K	16K	2K	4K
Tokens/Sec per Chip	473.3	69.7	8.1	4.3	2.7	8.6	7.0	26.5
TCO/1M Tokens (\$)	0.001	0.008	0.161	0.228	0.521	0.141	0.245	0.046

BLOOM [7], PaLM [9] and Llama-2 [55]. Details about these models are shown in Table 2. All studies were conducted on publicly released data, such as model architecture hyper-parameters, and do not use actual weights.

5.1 Design Space Exploration

We performed a thorough design exploration under 3 different context length scenarios (1024, 2048 and 4096) and on batch sizes from 1 to 1024. This exploration results in over 2 million valid design points for each model. Each design point combines the result from both hardware exploration and software evaluation, which includes hardware design (chip and server), software mapping (tensor parallelism size, pipeline parallelism size, batch size and micro-batch size), cost (OpEx and CapEx) and performance (latency and throughput), etc.

Table 2 shows the TCO/Token optimal Chiplet Cloud designs for each model in our case study. We found that all TCO-optimal designs are targeting batch sizes greater than or equal to 32. Large batch sizes are good for utilization in FC layers but will require additional silicon for memory to account for a larger KV cache. This means we either need bigger chips which greatly increase CapEx, or more chips which generate more inter-node traffic and hurt throughput. This will either result in larger chips which will sharply increase the CapEx as our silicon per chip gets larger and yield gets worse, or it will generate systems with a larger number of chips increasing the amount of inter-chip communication and diminishing the end-to-end performance. Finding batch sizes that balance each factor is essential to achieve good TCO/Token but is challenging to find. Each optimal design points across our 8 models all have different chip, server designs, and mapping strategies demonstrating the importance of our design methodology—every aspect of the system affects performance and cost and are sensitive to the requirements of the workload.

While the workload does impact the optimal Chiplet Cloud configuration, this doesn’t mean that a Chiplet Cloud instance can only run a single model. Additional discussion on the impact of

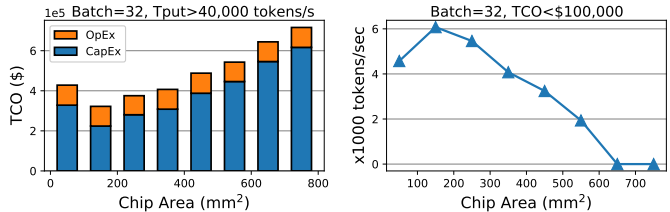


Figure 7: Proper chip size can reduce the fabrication costs (CapEx) without compromising performance as much. Left: For a given throughput requirement, chips with a size of less than 200 mm² have lowest TCO. Right: For a given TCO budget, chips with a size between 100 mm² to 200 mm² achieve the best throughput.

running non-optimized models and how a multi-model objective optimization perform can be found in Section 6.3.

5.2 Design Insights

How chip size affects TCO and performance. Figure 7 shows the results of GPT-3 in two different scenarios. On the left is how we should choose the die size to lower TCO for a given minimum throughput requirement. Compared to chips over 700 mm², which is the size of many traditional large monolithic chips, a chip around 200 mm² reduces TCO by about 2.2× and still meets the throughput constraint. We also find the CapEx exceeds 80% of TCO for most designs. The right side of Figure 7 shows chips with a size between 200 mm² to 300 mm² achieve the best throughput for a given TCO budget. This shows that proper chip sizing can effectively reduce TCO without compromising performance.

How the batch size affects TCO/Token. Figure 8 shows the TCO/1K Tokens versus batch size across 4 models and 3 context lengths. When the batch size is increased from 1, TCO/Tokens improves due to increases in compute utilization by providing more

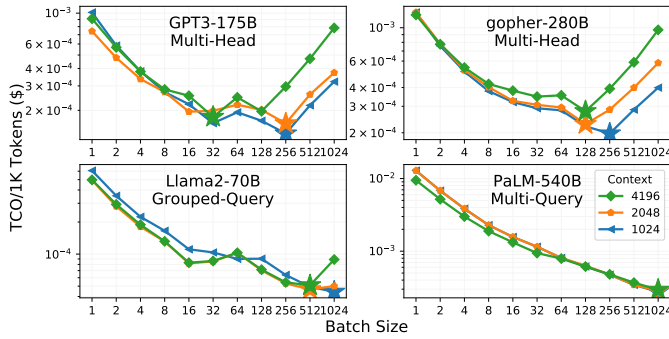


Figure 8: The optimal TCO/Token under different batch sizes. Small batch requires less silicon, and large batch benefits weight reuse. The optimal batch size for multi-head models is between 32 to 256, while the multi-query and grouped-query models are able to maintain a near-optimal TCO/Token at batch size 1024.

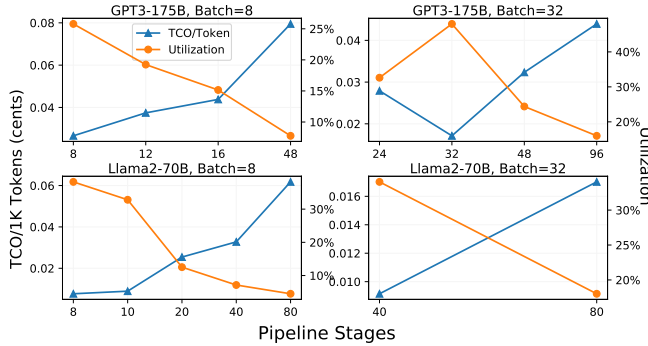


Figure 9: Pipeline stages sweeping for different models and batch sizes. The number of pipeline stages close to the batch size usually achieves the highest utilization, resulting in the optimal TCO/Token.

opportunities to exploit pipeline parallelism. As the batch size continues to increase, the utilization will reach a peak. For the traditional multi-head model, more silicon is required for KV cache in large batch size and long contexts, which significantly increases TCO/Token. Chiplet Cloud supports batch sizes up to 128 with near-optimal TCO/Token for these models. PaLM adopts multi-query attention [46] and Llama-2 adopts grouped-query attention [2], where key and value are shared across all or some groups of attention heads, which reduces the size of the KV cache by a factor of number of heads. For these models, Chiplet Cloud supports batch sizes up to 1024 with near-optimal TCO/Token. The cost of longer contexts is negligible, especially when the batch size is not too large.

How the mapping strategy affects TCO/Token for a given batch size. Figure 9 shows that when the number of pipeline stages p (i.e. the pipeline parallelism size) is close to the batch size, the system utilization is the largest and TCO/Token is optimal. When these two numbers are similar, the system can take full advantage

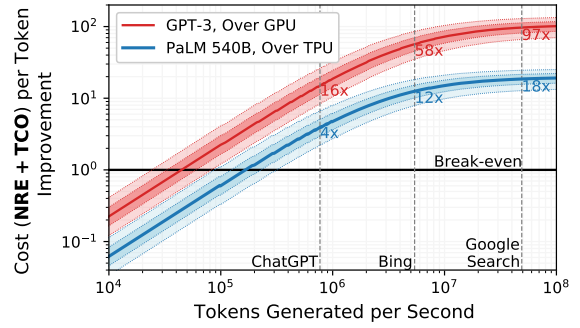


Figure 10: Compared to A100 GPU and TPUv4, Chiplet Cloud can achieve over 97× and 18× improvement in (NRE+TCO)/Token on GPT-3 and PaLM 540B, respectively. The light and dark shaded regions represent the results under $\pm 30\%$ and $\pm 15\%$ input variance.

of pipeline parallelism with a micro-batch size of 1, so the number of micro-batches is also close (if not equal) to the pipeline stage [3]. This helps balance the latency of micro-batches passing through all pipeline stages and pipeline stages completing all micro-batches. This finding aligns with our inference simulation discussed in Section 4.2. Specifically, when p is too small, performance is hindered by pipeline stage latency, whereas an excessively large p results in limitation by microbatch latency.

6 Evaluation

In this section, we evaluate the performance and cost of Chiplet Cloud for serving large language models. The key metric we are targeting is $TCO/Token$. TCO/Token is measured as cost per token generated and is the key factor in the ability to democratize LLMs. One of the most popular business models for generative LLMs is also to charge users per generated token. Lower TCO/Token not only adds more profit margins, but also makes LLMs more approachable. We compare Chiplet Cloud to state-of-the-art GPU and TPU cloud implementations. We also evaluate the sparsity support and flexibility of Chiplet Cloud architectures.

6.1 Comparison with GPUs and TPUs.

We compare optimal Chiplet Cloud designs from Section 5 to state-of-the-art A100 GPU [3] and TPUv4 [37] implementations. Neither work is specifically optimized for TCO/Token. For our comparison, we choose the throughput optimal result for GPU, and the utilization optimal result for TPU, which are key indicators that you are close to TCO/Token optimal. Compared to GPU and TPU clouds, our design achieves up to 106.0× and 19.9× TCO/Token improvement on GPT-3 and PaLM 540B respectively. TCO for GPUs and TPUs are based on the best cloud rental price we could find [10, 26].

Adding the NRE of Chiplet Cloud (\$35M, estimated based on the NRE model from Moonwalk [24]), we show the actual cost improvement in Figure 10. As the number of tokens expected to be generated (x-axis) grow, NRE is greatly amortized and Chiplet Cloud gains more improvement over GPU and TPU. Compared to A100 GPU and TPUv4 clouds, at the scale of Google search (99,000 queries per

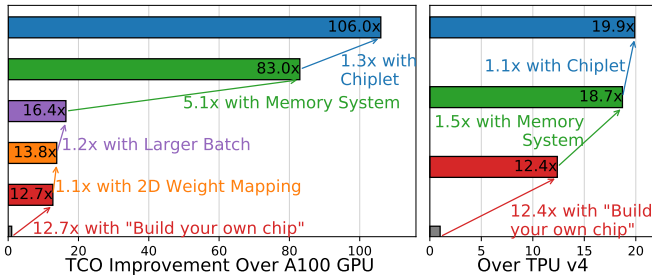


Figure 11: TCO/Token improvement breakdown over GPU and TPU.

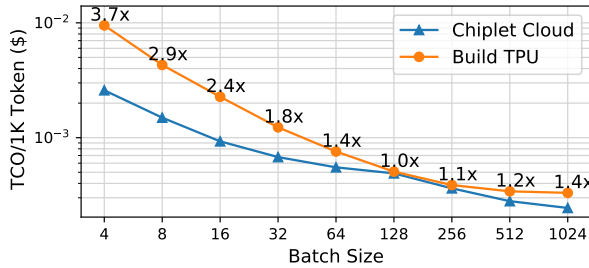


Figure 12: Chiplot Cloud is more efficient than TPU v4 at most batch sizes, especially for small batch sizes. TPU performance is from [37] with and TCO is from our model.

second [30], and assuming 500 tokens per query), Chiplot Cloud achieves 97× and 18× improvement on (TCO+NRE)/Token, respectively. We also add variance to 2 inputs that are difficult to accurately estimate, those being the TCO of GPU and TPU clouds, and the NRE of Chiplot Cloud. With a ±30% variance of these inputs, Chiplot Cloud is still expected to maintain a 66× to 129× improvement over GPU, and 12× to 24× improvement over TPU.

Figure 11 shows the breakdown of TCO/Token of Chiplot Cloud over GPU and TPU. Some of the improvement in TCO comes from building the silicon instead of renting it. To analyze the impact of owning a chip, we feed the chip and server specifications of A100 and TPU v4 into our TCO model. The results show that owing the chip saves 12.7× and 12.4× in TCO/Token. Note that the actual savings should be less than this, as our model does not include the cost of liquid cooling and advanced packaging, which are critical for TPUs and GPUs but not required for Chiplot Cloud. We see that our specialized memory system improves TCO/Token by 5.1× and 1.5× over GPUs and TPUs, while die sizing improves it by an additional 1.3× and 1.1×. Compared to GPUs, the 2D weight-stationary layout in feed-forward network and the larger batch sizes lead to a 1.1× and 1.2× improvement respectively. Both of these optimizations are supported in the TPU implementation.

In Figure 12, we compare the architectural benefits of Chiplot Cloud versus TPU v4 [37] using our model for the TPU’s TCO. Chiplot Cloud is more efficient at most batch sizes and achieves a TCO/Token improvement of up to 3.7× at batch size 4 as the high-bandwidth CC-MEM benefits from low operational intensity.

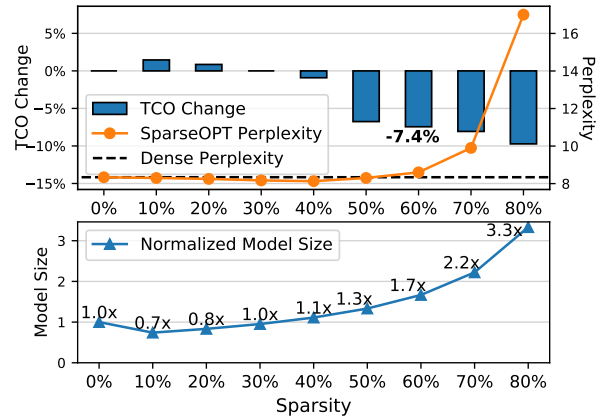


Figure 13: Top: TCO/Token and perplexity (from SparseGPT [15], lower is better) of OPT-175B under different sparsity. Chiplot Cloud can further reduce 7.4% of TCO/Token at 60% sparsity with negligible increase in perplexity. Bottom: Chiplot Cloud supports a 1.7× larger model with a sparsity of 60%.

6.2 Sparse Models Evaluation

We evaluate the sparse models in Figure 13. The top plot compares TCO and perplexity of OPT-175B [62] under different weight sparsities. The perplexity values are from SparseGPT [15]. The blue bars show the change in TCO/Token compared to using the non-compressed dense model. At low sparsity (such as 10% and 20%), TCO/Token increases because it requires more memory to store compressed format encoding overhead. 60% sparsity represents a sweet spot where the perplexity of the model is only marginally above that of the dense model while attaining a 7.4% improvement in TCO/Token. Additional sparsity continues to give additional improvements in TCO but the model perplexity starts to increase rapidly. Chiplot Cloud also supports larger models with sparsity. The bottom of Figure 13 shows that under the same system configuration, Chiplot Cloud is able to support models with 1.7× parameters at a sparsity of 60%.

6.3 Chiplot Cloud Flexibility

Flexibility is one of the main limiting factors for large-scale deployment of ASIC supercomputers. ASIC designs with higher flexibility are believed to have longer lifetimes and thus easier to amortize the NRE costs. The main flexibility of Chiplot Cloud depends on the flexibility of chip design, which usually dominates in NRE. It is feasible to redesign servers and software mapping for different generative language models using the same chip. Since LLM scaling changes the number of parameters, while the operational intensity usually remains the same, Chiplot Cloud is able to support LLMs of larger sizes by adding chips. LLMs may also have different element-wise operations, such as different activation functions and positional embeddings, our highly programmable SIMD cores are able to support all of these variations.

By adjusting the number of chips and optimizing the server and mapping, one chip design can run models of different sizes

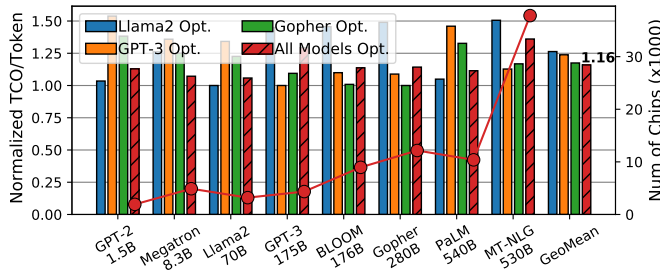


Figure 14: A Chiplet Cloud chip design is flexible to run models of different sizes via scale-up. Comparing to the model-optimized design, chip optimized for other models has TCO/Token of $1.1\times$ to $1.5\times$ (blue, orange and green bar). One can also optimize the chip for multi-model (dashed red bars) at only $1.16\times$ TCO/Token on average, and the number of chips used is shown in red dots.

without sacrificing too much TCO/Token. In Figure 14, we show the impact on TCO/Token when mapping a chip to different models. We first show 3 model-optimized chip designs in blue, orange and green bars for Llama2, Gopher, and GPT-3, respectively. When running different models, it only increases TCO/Token by $1.1\times$ to $1.5\times$ compared to the corresponding model-optimized design. When flexibility comes as the first priority, one can also set a multi-model optimization for the chip design. The red dashed box shows a design optimized for the geometric mean of TCO/Token on all 8 models, achieving an average overhead of only $0.16\times$ compared to the 8 single-model optimized designs. The red dots represent the number of chips used for each model. This demonstrates Chiplet Cloud has the flexibility to support various LLMs.

6.4 NRE Discussion

One major factor limiting the deployment of ASICs is non-recurring engineering (NRE) costs [24]. The barrier for overcoming NRE is primarily about the opportunity cost of running the workload on the current hardware offerings. The difference in TCO between running a workload on an ASIC supercomputer vs the current available hardware platform determines the break even point for NRE, where the NRE cost directly equals the savings from using an ASIC supercomputer. Figure 15 shows the minimum required TCO/Token improvement in order to justify the NRE. We extend the NRE model from Moonwalk [24] to use a 7nm technology node and estimate the NRE of an ASIC accelerator for large language models to be approximately \$35M, including silicon mask cost, CAD tools, IP licensing, flip-chip BGA packing, server designs, and labor. Even if it were \$100M, the current cost of running workloads like ChatGPT and web search with integrated LLMs is so massive that it not only justifies the cost of creating ASIC supercomputers but going even further as to co-optimize those supercomputers for specific LLMs for additional improvement in TCO per token. This shows that the NRE cost of ASIC supercomputers is justifiable for modern workloads and thus customized hardware still remains the best solution to democratize LLMs.

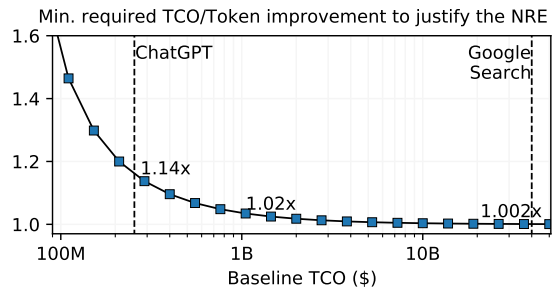


Figure 15: Designing ASIC for LLMs will be more cost-effective than using GPUs since the demand is so high. ChatGPT using GPUs has a TCO of \$255 M [31] per year, requiring only a $1.14\times$ TCO/Token improvement of ASIC to justify the NRE costs.

7 Related Work

Cloud-scale acceleration and TCO optimization. Microsoft’s Brainwave [14] proposes FPGA-based clouds for ML. Google’s TPU [20] ML cloud is designed for performance per TCO. Magaki et al [29] proposes ASIC Clouds for scale-out application with TCO optimization. Moonwalk [24] optimizes the NRE for ASIC Clouds.

Training and serving large language models. Megatron-LM [48] and DeepSpeed [3, 43] proposes multi-GPU training and inference solution to minimize latency while maximizing throughput. [33] improves pipeline parallelism and combines it with Megatron-LM and achieves high aggregate throughput. PaLM [9] train a 540B parameter model on 6144 TPUv4 chips using Pathways [5]. Pope et al [37] optimizes large scale transformer inference on TPUv4.

ASIC accelerators for transformer models. ELSA [17] presents an approximation scheme for the attention mechanism. SpAtten [59] exploits the token and head sparsity and quantization opportunities in the attention block. EdgeBERT [53] leverages dynamic voltage-frequency scaling based on early exit prediction of ALBERT [27]. FLAT [23] optimizes the dataflow in attention. CTA [58] proposes a HW-SW co-design for attention compression.

8 Conclusion

This paper presents Chiplet Cloud, a chiplet-based ASIC LLM-supercomputer architecture that achieves unprecedented TCO/Token for serving large generative language model. It employs an on-chip memory architecture, CC-MEM, to eliminate bandwidth limitations, and a compression decoder for supporting sparse models, while moderating the die size to improve system costs. We also propose a comprehensive design methodology that accurately explores Chiplet Cloud’s design space. We design Chiplet Cloud systems for eight language models and achieved up to $97\times$ and $18\times$ better TCO/Token compared to running on GPU and TPU cloud, respectively. We believe Chiplet Cloud to be the best solution to democratize modern and future large generative language models.

Acknowledgements

This work was supported by NSF Award 2118628.

References

- [1] Abien Fred Agarap. 2019. Deep Learning using Rectified Linear Units (ReLU). *arXiv:1803.08375 [cs]* (2019).
- [2] Joshua Ainslie, James Lee-Thorp, Michiel de Jong, Yury Zemlyanskiy, Federico Lebrón, and Sumit Sanghai. 2023. GQA: Training Generalized Multi-Query Transformer Models from Multi-Head Checkpoints. *arXiv:2305.13245 [cs]* (2023).
- [3] Reza Yazdani Aminabadi, Samyam Rajbhandari, Ammar Ahmad Awan, Cheng Li, Du Li, Elton Zheng, Olatunji Ruwase, Shaden Smith, Minjia Zhang, Jeff Rasley, and Yuxiong He. 2022. DeepSpeed-Inference: Enabling Efficient Inference of Transformer Models at Unprecedented Scale. In *Proceedings of the International Conference for High Performance Computing, Networking, Storage and Analysis (SC)*.
- [4] Jimmy Lei Ba, Jamie Ryan Kiros, and Geoffrey E. Hinton. 2016. Layer Normalization. *arXiv:1607.06450 [stat]* (2016).
- [5] Paul Barham, Aakanksha Chowdhery, Jeff Dean, Sanjay Ghemawat, Steven Hand, Dan Hurt, Michael Isard, Hyeontaek Lim, Ruoming Pang, Sudip Roy, Brennan Saeta, Parker Schuh, Ryan Sepassi, Laurent El Shafey, Chandramohan A. Thekkath, and Yonghui Wu. 2022. Pathways: Asynchronous Distributed Dataflow for ML. *arXiv:2203.12533 [cs]* (2022).
- [6] Luiz André Barroso, Urs Hölzle, and Parthasarathy Ranganathan. 2013. The Datacenter as a Computer: Designing Warehouse-Scale Machines. *Synthesis lectures on computer architecture* (2013).
- [7] BigScience. 2023. BLOOM: A 176B-Parameter Open-Access Multilingual Language Model. *arXiv:2211.05100 [cs]* (2023).
- [8] Tom B. Brown, Benjamin Mann, Nick Ryder, Melanie Subbiah, Jared Kaplan, Prafulla Dhariwal, Arvind Neelakantan, Pranav Shyam, Girish Sastry, Amanda Askell, Sandhini Agarwal, Ariel Herbert-Voss, Gretchen Krueger, Tom Henighan, Rewon Child, Aditya Ramesh, Daniel M. Ziegler, Jeffrey Wu, Clemens Winter, Christopher Hesse, Mark Chen, Eric Sigler, Mateusz Litwin, Scott Gray, Benjamin Chess, Jack Clark, Christopher Berner, Sam McCandlish, Alec Radford, Ilya Sutskever, and Dario Amodei. 2020. Language Models are Few-Shot Learners. *arXiv:2005.14165 [cs]* (2020).
- [9] Aakanksha Chowdhery, Sharan Narang, Jacob Devlin, Maarten Bosma, Gaurav Mishra, Adam Roberts, Paul Barham, Hyung Won Chung, Charles Sutton, Sebastian Gehrmann, Parker Schuh, Kensen Shi, Sasha Tsvyashchenko, Joshua Maynez, Abhishek Rao, Parker Barnes, Yi Tay, Noam Shazeer, Vinodkumar Prabhakaran, Emily Reif, Nan Du, Ben Hutchinson, Reiner Pope, James Bradbury, Jacob Austin, Michael Isard, Guy Gur-Ari, Pengcheng Yin, Toju Duke, Anselm Levskaya, Sanjay Ghemawat, Sunipa Dev, Henryk Michalewski, Xavier Garcia, Vedant Misra, Kevin Robinson, Liam Fedus, Denny Zhou, Daphne Ippolito, David Luan, Hyeontaek Lim, Barret Zoph, Alexander Spiridonov, Ryan Sepassi, David Dohan, Shivani Agrawal, Mark Omernick, Andrew M. Dai, Thanumalayan Sankaranarayanan Pillai, Marie Pellat, Aitor Lewkowycz, Erica Moreira, Rewon Child, Oleksandr Polozov, Katherine Lee, Zongwei Zhou, Xuezhi Wang, Brennan Saeta, Mark Diaz, Orhan Firat, Michele Catasta, Jason Wei, Kathy Meier-Hellstern, Douglas Eck, Jeff Dean, Slav Petrov, and Noah Fiedel. 2022. PaLM: Scaling Language Modeling with Pathways. *arXiv:2204.02311 [cs]* (2022).
- [10] Google Cloud. 2023. Cloud TPU Pricing. <https://cloud.google.com/tpu/pricing#v4-pricing>. <https://cloud.google.com/tpu/pricing#v4-pricing>
- [11] CNET. 2021. Gigawatt: The solar energy term you should know about. <https://www.cnet.com/home/energy-and-utilities/gigawatt-the-solar-energy-term-you-should-know-about/>.
- [12] J.A. Cunningham. 1990. The use and evaluation of yield models in integrated circuit manufacturing. *IEEE Transactions on Semiconductor Manufacturing* (1990).
- [13] William Fedus, Barret Zoph, and Noam Shazeer. 2021. Switch Transformers: Scaling to Trillion Parameter Models with Simple and Efficient Sparsity. *arXiv:2101.03961 [cs]* (2021).
- [14] Jeremy Fowers, Kalin Ovtcharov, Michael Papamichael, Todd Massengill, Ming Liu, Daniel Lo, Shlomi Alkalay, Michael Haselman, Logan Adams, Mahdi Ghandi, Stephen Heil, Prerak Patel, Adam Sapek, Gabriel Weisz, Lisa Woods, Sitaram Lanka, Steven K. Reinhardt, Adrian M. Caulfield, Eric S. Chung, and Doug Burger. 2018. A Configurable Cloud-Scale DNN Processor for Real-Time AI. In *Proceedings of the 45th International Symposium on Computer Architecture (ISCA)*.
- [15] Elias Frantar and Dan Alistarh. 2023. SparseGPT: Massive Language Models Can Be Accurately Pruned in One-Shot. *arXiv:2301.00774 [cs]* (2023).
- [16] GitHub. 2023. GitHub Copilot Your AI Pair Programmer. <https://github.com/features/copilot>.
- [17] Tae Jun Ham, Yejin Lee, Seong Hoon Seo, Soosung Kim, Hyunji Choi, Sung Jun Jung, and Jae W. Lee. 2021. ELSA: Hardware-Software Co-design for Efficient, Lightweight Self-Attention Mechanism in Neural Networks. In *Proceedings of the 48th International Symposium on Computer Architecture (ISCA)*.
- [18] Dan Hendrycks and Kevin Gimpel. 2023. Gaussian Error Linear Units (GELUs). *arXiv:1606.08415 [cs]* (2023).
- [19] Norman P. Jouppi, George Kurian, Sheng Li, Peter Ma, Rahul Nagarajan, Lifeng Nai, Nishant Patil, Suvinay Subramanian, Andy Swing, Brian Towles, et al. 2023. TPU v4: An optically reconfigurable supercomputer for machine learning with hardware support for embeddings. In *Proceedings of the International Symposium on Computer Architecture (ISCA)*.
- [20] Norman P. Jouppi, Doe Hyun Yoon, Matthew Ashcraft, Mark Gottscho, Thomas B. Jablin, George Kurian, James Laudon, Sheng Li, Peter Ma, Xiaoyu Ma, Thomas Norrie, Nishant Patil, Sushma Prasad, Cliff Young, Zongwei Zhou, and David Patterson. 2021. Ten Lessons From Three Generations Shaped Google's TPUv4: Industrial Product. In *Proceedings of the 48th International Symposium on Computer Architecture (ISCA)*.
- [21] Norman P. Jouppi, Doe Hyun Yoon, George Kurian, Sheng Li, Nishant Patil, James Laudon, Cliff Young, and David Patterson. 2020. A Domain-specific Supercomputer for Training Deep Neural Networks. *Commun. ACM* (2020).
- [22] Ajaykumar Kannan, Natalie Enright Jerger, and Gabriel H. Loh. 2015. Enabling Interposer-based Disintegration of Multi-core Processors. In *Proceedings of the 48th International Symposium on Microarchitecture (MICRO)*.
- [23] Sheng-Chun Kao, Suvinay Subramanian, Gaurav Agrawal, Amir Yazdanbakhsh, and Tushar Krishna. 2023. FLAT: An Optimized Dataflow for Mitigating Attention Bottlenecks. In *Proceedings of the International Conference on Architectural Support for Programming Languages and Operating Systems (ASPLOS)*.
- [24] Moein Khazraee, Lu Zhang, Luis Vega, and Michael Bedford Taylor. 2017. Moonwalk: NRE Optimization in ASIC Clouds. In *Proceedings of the 22nd International Conference on Architectural Support for Programming Languages and Operating Systems (ASPLOS)*.
- [25] Simon Knowles. 2021. Graphcore Colossus Mk2 IPU. In *Hot Chips 33 Symposium*.
- [26] Lambda. 2023. The Best Prices for Cloud GPUs. <https://lambdalabs.com/service/gpu-cloud>.
- [27] Zhenzhong Lan, Mingda Chen, Sebastian Goodman, Kevin Gimpel, Piyush Sharma, and Radu Soricut. 2020. ALBERT: A Lite BERT for Self-supervised Learning of Language Representations. *arXiv:1909.11942 [cs]* (2020).
- [28] Ryan Liu and Chuang Feng. 2021. AI Compute Chip from Enflame. In *Hot Chips 33 Symposium*.
- [29] Ikuo Magaki, Moein Khazraee, Luis Vega Gutierrez, and Michael Bedford Taylor. 2016. ASIC Clouds: Specializing the Datacenter. In *Proceedings of the 43rd International Symposium on Computer Architecture (ISCA)*.
- [30] Maryam Mohsin. 2023. 10 Google Search Statistics You Need to Know in 2023. <https://www.oberlo.com/blog/google-search-statistics#:~:text=We%20know%20that%20there%20are,Internet%20Live%20Stats%2C%202022>.
- [31] Aaron Mok. 2023. ChatGPT could cost over \$700,000 per day to operate. Microsoft is reportedly trying to make it cheaper. <https://www.businessinsider.com/how-much-chatgpt-costs-openai-to-run-estimate-report-2023-4>.
- [32] Samuel Naffziger, Noah Beck, Thomas Burd, Kevin Lepak, Gabriel H. Loh, Mahesh Subramony, and Sean White. 2021. Pioneering Chiplet Technology and Design for the AMD EPYC™ and Ryzen™ Processor Families: Industrial Product. In *Proceedings of the 48th Annual International Symposium on Computer Architecture (ISCA)*.
- [33] Deepak Narayanan, Mohammad Shoeybi, Jared Casper, Patrick LeGresley, Mostofa Patwary, Vijay Korthikanti, Dmitri Vainbrand, Prethvi Kashinkunti, Julie Bernauer, Bryan Catanzaro, Amar Phanishayee, and Matei Zaharia. 2021. Efficient large-scale language model training on GPU clusters using megatron-LM. In *Proceedings of the International Conference for High Performance Computing, Networking, Storage and Analysis (SC)*.
- [34] Yuyao Niu, Zhengyang Lu, Meichen Dong, Zhou Jin, Weifeng Liu, and Guangming Tan. 2021. TileSpMV: A Tiled Algorithm for Sparse Matrix-Vector Multiplication on GPUs. In *IEEE International Parallel and Distributed Processing Symposium (IPDPS)*.
- [35] OpenAI. 2022. Introducing ChatGPT. <https://openai.com/blog/chatgpt>.
- [36] Daniel Petrisco, Chun Zhao, Scott Davidson, Paul Gao, Dustin Richmond, and Michael Bedford Taylor. 2020. NoC Symbiosis. In *IEEE/ACM International Symposium on Networks-on-Chip (NOCS)*.
- [37] Reiner Pope, Sholto Douglas, Aakanksha Chowdhery, Jacob Devlin, James Bradbury, Anselm Levskaya, Jonathan Heek, Kefan Xiao, Shivani Agrawal, and Jeff Dean. 2022. Efficiently Scaling Transformer Inference. *arXiv:2211.05102 [cs]* (2022).
- [38] John W. Poulton, John M. Wilson, Walker J. Turner, Brian Zimmer, Xi Chen, Sudhir S. Kudva, Sanquan Song, Stephen G. Tell, Nikola Nedovic, Wenxu Zhao, Sunil R. Sudhakaran, C. Thomas Gray, and William J. Dally. 2019. A 1.17-pJ/b, 25-Gb/s/pin Ground-Referenced Single-Ended Serial Link for Off- and On-Package Communication Using a Process- and Temperature-Adaptive Voltage Regulator. *IEEE Journal of Solid-State Circuits* (2019).
- [39] Raghu Prabhakar and Sumti Jairath. 2021. SambaNova SN10 RDU: Accelerating Software 2.0 with Dataflow. In *Hot Chips 33 Symposium*.
- [40] Ofir Press, Noah A. Smith, and Mike Lewis. 2022. Train Short, Test Long: Attention with Linear Biases Enables Input Length Extrapolation. *arXiv:2108.12409 [cs]* (2022).
- [41] Alec Radford, Jeffrey Wu, Rewon Child, David Luan, Dario Amodei, Ilya Sutskever, et al. 2019. Language Models are Unsupervised Multitask Learners. *OpenAI blog* (2019).
- [42] Jack W. Rae, Sebastian Borgeaud, Trevor Cai, Katie Millican, Jordan Hoffmann, Francis Song, John Aslanides, Sarah Henderson, Roman Ring, Susannah Young, Eliza Rutherford, Tom Hennigan, Jacob Menick, Albin Cassier, Richard Powell,

- George van den Driessche, Lisa Anne Hendricks, Maribeth Rauh, Po-Sen Huang, Amelia Glaese, Johannes Welbl, Sumanth Dathathri, Saffron Huang, Jonathan Uesato, John Mellor, Irina Higgins, Antonia Creswell, Nat McAleese, Amy Wu, Erich Elsen, Siddhant Jayakumar, Elena Buchatskaya, David Budden, Esmé Sutherland, Karen Simonyan, Michela Paganini, Laurent Sifre, Lena Martens, Xiang Lorraine Li, Adhiguna Kuncoro, Aida Nematzadeh, Elena Gribovskaya, Domenic Donato, Angeliki Lazaridou, Arthur Mensch, Jean-Baptiste Lespiau, Maria Tsimpoukelli, Nikolai Grigorev, Doug Fritz, Thibault Sottiaux, Mantas Pajarskas, Toby Pohlen, Zhitao Gong, Daniel Toyama, Cyprien de Masson d’Autume, Yujia Li, Tayfun Terzi, Vladimir Mikulik, Igor Babuschkin, Aidan Clark, Diego de Las Casas, Aurelia Guy, Chris Jones, James Bradbury, Matthew Johnson, Blake Hechtman, Laura Weidinger, Iason Gabriel, William Isaac, Ed Lockhart, Simon Osindero, Laura Rimell, Chris Dyer, Oriol Vinyals, Kareem Ayoub, Jeff Stanway, Lorraine Bennett, Demis Hassabis, Koray Kavukcuoglu, and Geoffrey Irving. 2022. Scaling Language Models: Methods, Analysis & Insights from Training Gopher. *arXiv:2112.11446 [cs]* (2022).
- [43] Samyam Rajbhandari, Conglong Li, Zhewei Yao, Minjia Zhang, Reza Yazdani Aminabadi, Ammar Ahmad Awan, Jeff Rasley, and Yuxiong He. 2022. DeepSpeed-MoE: Advancing Mixture-of-Experts Inference and Training to Power Next-Generation AI Scale. *arXiv:2201.05596 [cs]* (2022).
- [44] Prajit Ramachandran, Barret Zoph, and Quoc V. Le. 2017. Searching for Activation Functions. *arXiv:1710.05941 [cs]* (2017).
- [45] Peter Shaw, Jakob Uszkoreit, and Ashish Vaswani. 2018. Self-Attention with Relative Position Representations. *arXiv:1803.02155 [cs]* (2018).
- [46] Noam Shazeer. 2019. Fast Transformer Decoding: One Write-Head is All You Need. *arXiv:1911.02150 [cs]* (2019).
- [47] Noam Shazeer. 2020. GLU Variants Improve Transformer. *arXiv:2002.05202 [cs]* (2020).
- [48] Mohammad Shoeybi, Mostofa Patwary, Raul Puri, Patrick LeGresley, Jared Casper, and Bryan Catanzaro. 2020. Megatron-LM: Training Multi-Billion Parameter Language Models Using Model Parallelism. *arXiv:1909.08053 [cs]* (2020).
- [49] Misha Smelyanskiy. 2019. Zion: Facebook Next- Generation Large Memory Training Platform. In *Hot Chips 31 Symposium*.
- [50] Shaden Smith, Mostofa Patwary, Brandon Norick, Patrick LeGresley, Samyam Rajbhandari, Jared Casper, Zhun Liu, Shrimai Prabhunoye, George Zerveas, Vijay Korthikanti, Elton Zhang, Rewon Child, Reza Yazdani Aminabadi, Julie Bernauer, Xia Song, Mohammad Shoeybi, Yuxiong He, Michael Houston, Saurabh Tiwary, and Bryan Catanzaro. 2022. Using DeepSpeed and Megatron to Train Megatron-Turing NLG 530B, A Large-Scale Generative Language Model. *arXiv:2201.11990 [cs]* (2022).
- [51] Jianlin Su, Yu Lu, Shengfeng Pan, Ahmed Murtadha, Bo Wen, and Yunfeng Liu. 2022. RoFormer: Enhanced Transformer with Rotary Position Embedding. *arXiv:2104.09864 [cs]* (2022).
- [52] Cerebras Systems. 2019. Wafer-Scale Deep Learning. In *Hot Chips 31 Symposium*.
- [53] Thierry Tambe, Coleman Hooper, Lillian Pentecost, Tianyu Jia, En-Yu Yang, Marco Donato, Victor Sanh, Paul Whatmough, Alexander M. Rush, David Brooks, and Gu-Yeon Wei. 2021. EdgeBERT: Sentence-Level Energy Optimizations for Latency-Aware Multi-Task NLP Inference. In *Proceedings of the 54th International Symposium on Microarchitecture (MICRO)*.
- [54] TechPowerUp. 2023. NVIDIA A100 SXM4 40 GB. <https://www.techpowerup.com/gpu-specs/a100-sxm4-40-gb.c3506>.
- [55] Hugo Touvron, Louis Martin, Kevin Stone, Peter Albert, Amjad Almahairi, Yasmine Babaei, Nikolay Bashlykov, Soumya Batra, Prajwal Bhargava, Shruti Bhosale, Dan Bikel, Lukas Blecher, Cristian Canton Ferrer, Moya Chen, Guillem Cucurull, David Esiobu, Jude Fernandes, Jeremy Fu, Wenyin Fu, Brian Fuller, Cynthia Gao, Vedanuj Goswami, Naman Goyal, Anthony Hartshorn, Saghar Hosseini, Rui Hou, Hakan Inan, Marcin Kardas, Viktor Kerkez, Madian Khabsa, Isabel Kloumann, Artem Korenev, Punit Singh Koura, Marie-Anne Lachaux, Thibaut Lavril, Jenya Lee, Diana Liskovich, Yinghai Lu, Yuning Mao, Xavier Martinet, Todor Mihaylov, Pushkar Mishra, Igor Molybog, Yixin Nie, Andrew Poulton, Jeremy Reizenstein, Rashi Rungta, Kalyan Saladi, Alan Schelten, Ruan Silva, Eric Michael Smith, Ranjan Subramanian, Xiaoqing Ellen Tan, Binh Tang, Ross Taylor, Adina Williams, Jian Xiang Kuan, Puxin Xu, Zheng Yan, Iliyan Zarov, Yuchen Zhang, Angela Fan, Melanie Kambadur, Sharan Narang, Aurelien Rodriguez, Robert Stojnic, Sergey Edunov, and Thomas Scialom. 2023. Llama 2: Open Foundation and Fine-Tuned Chat Models. *arXiv:2307.09288 [cs]* (2023). *arXiv:2307.09288 [cs.CL]*
- [56] Walker J. Turner, John W. Poulton, John M. Wilson, Xi Chen, Stephen G. Tell, Matthew Fojtik, Thomas H. Greer, Brian Zimmer, Sanquan Song, Nikola Nedovic, Sudhir S. Kudva, Sunil R. Sudhakaran, Rizwan Bashirullah, Wenxu Zhao, William J. Dally, and C. Thomas Gray. 2018. Ground-referenced Signaling for Intra-chip and Short-reach Chip-to-chip Interconnects. In *Custom Integrated Circuits Conference (CICC)*.
- [57] Ashish Vaswani, Noam Shazeer, Niki Parmar, Jakob Uszkoreit, Llion Jones, Aidan N. Gomez, Lukasz Kaiser, and Illia Polosukhin. 2017. Attention Is All You Need. *arXiv:1706.03762 [cs]* (2017).
- [58] Haoran Wang, Haobo Xu, Ying Wang, and Yinhe Han. 2023. CTA: Hardware-Software Co-design for Compressed Token Attention Mechanism. In *International Symposium on High-Performance Computer Architecture (HPCA)*.
- [59] Hanrui Wang, Zhekai Zhang, and Song Han. 2021. SpAtten: Efficient Sparse Attention Architecture with Cascade Token and Head Pruning. *arXiv:2012.09852 [cs]* (2021).
- [60] WikiChip. 2022. 7 nm Lithography Process. https://en.wikichip.org/wiki/7_nm_lithography_process.
- [61] Biao Zhang and Rico Sennrich. 2019. Root Mean Square Layer Normalization. *arXiv:1910.07467 [cs]* (2019).
- [62] Susan Zhang, Stephen Roller, Naman Goyal, Mikel Artetxe, Moya Chen, Shuohui Chen, Christopher Dewan, Mona Diab, Xian Li, Xi Victoria Lin, Todor Mihaylov, Myle Ott, Sam Shleifer, Kurt Shuster, Daniel Simig, Punit Singh Koura, Anjali Sridhar, Tianlu Wang, and Luke Zettlemoyer. 2022. OPT: Open Pre-trained Transformer Language Models. *arXiv:2205.01068 [cs]* (2022).